Analysis of a Chinese hamster ovary cell mutant with defective mobilization of cholesterol from the plasma membrane to the endoplasmic reticulum

Natalie L. Jacobs,* Biree Andemariam,* Kathryn W. Underwood,* Krishnanchali Panchalingam,* David Sternberg,† Margaret Kielian,† and Laura Liscum[1,]*

Department of Physiology,* Tufts University School of Medicine, Boston, MA 02111, and Department of Cell Biology,† Albert Einstein College of Medicine, Bronx, NY 10461

Abstract The factors involved in shuttling cholesterol among cellular membranes have not been defined. Using amphotericin B selection, we previously isolated Chinese hamster ovary cell mutants expressing defects in intracellular cholesterol transport. Complementation analysis among seven mutants identified one cell line, mutant 3-6, with a unique defect. The present analysis revealed three key features of mutant 3-6. First, the movement of cholesterol both from the endoplasmic reticulum and through lysosomes to the plasma membrane was normal. However, when intact 3-6 cells were treated with sphingomyelinase, movement of plasma membrane cholesterol to acyl CoA: cholesterol acyltransferase in the endoplasmic reticulum was defective. Cellular cholesterol was mobilized to this enzyme upon activation by 25-hydroxycholesterol. Second, mutant 3-6 did not utilize endogenously synthesized sterol or low density lipoprotein-derived cholesterol for growth as effectively as parental Chinese hamster ovary cells. Finally, despite normal movement of cholesterol to the plasma membrane, mutant 3-6 was amphotericin B resistant. The plasma membrane cholesterol content was normal as assessed by cholesterol oxidase treatment and Semliki Forest virus fusion, which suggests that the 3-6 mutation alters the organization of cholesterol in the plasma membrane. Our characterization of this mutant cell line should facilitate the identification of gene(s) required for this transport pathway.—**Jacobs, N. L., B. Andemariam, K. W. Underwood, K. Panchalingam, D. Sternberg, M. Kielian, and L. Liscum.** Analysis of a Chinese hamster ovary cell mutant with defective mobilization of cholesterol from the plasma membrane to the endoplasmic reticulum. *J. Lipid Res.* 1997. **38:** 1973–1987.

Supplementary key words somatic cell mutant • low density lipoprotein • sphingomyelinase

The distribution of cholesterol in mammalian cells is tightly controlled. At steady state, most cellular cholesterol resides in the plasma membrane (1, 2), where it plays an essential role in maintaining membrane fluidity. The factors that maintain high cholesterol levels in the plasma membrane are not clear. The plasma membrane is also sphingomyelin-enriched, and there is evidence that cholesterol and sphingomyelin contents are linked (3–5). However, the sphingomyelin content alone cannot account for the plasma membrane's cholesterol level (6).

In addition, the cellular factors involved in shuttling cholesterol between the plasma membrane and intracellular membranes have not been defined. Nascent cholesterol, synthesized in the endoplasmic reticulum (ER), and low density lipoprotein (LDL) cholesterol, derived from hydrolysis of LDL-cholesteryl esters in the lysosome, are transported rapidly to the plasma membrane (7–9). Once in the plasma membrane, cholesterol appears to be in dynamic equilibrium with intracellular membranes, and it has been estimated that the cellular cholesterol pool moves continuously between the plasma membrane and ER (10).

We have taken a somatic cell genetic approach to identifying gene products involved in intracellular cholesterol transport. Chinese hamster ovary (CHO) cells were mutagenized and subjected to a selection protocol designed to isolate cells expressing defects in the transport of LDL-derived cholesterol from lysosomes to the plasma membrane (11). Several of the mutants had the desired biochemical phenotype, which resembles classic Niemann-Pick disease type C (NPC). NPC fibroblasts exhibit lysosomal storage of unesterified cholesterol due to a single gene defect that affects the egress of

Abbreviations: ER, endoplasmic reticulum; LDL, low density lipoprotein; CHO, Chinese hamster ovary; NPC, Niemann-Pick type C; ced, cholesterol esterification defective; 25-HC, 25-hydroxycholesterol; CL, cholesteryl linoleate; BSA, bovine serum albumin; TLC, thin-layer chromatography; SFV, Semliki Forest virus; HMG, 3-hydroxy-3-methylglutaryl; ACAT, acyl-CoA: cholesterol acyltransferase; EBSS, Earle's balanced salt solution.

[1]To whom correspondence should be addressed.

LDL-cholesterol from lysosomes and LDL-mediated regulation of cellular cholesterol homeostasis (12–15). The underlying NPC gene defect is unknown, although the defect has been linked to human chromosome 18 (16).

For each mutant tested, the ability of LDL to stimulate cholesterol esterification was found to be profoundly defective. Therefore, the mutant classes were termed cholesterol esterification defective (ced). Complementation analysis was carried out among six of our mutant lines and CT, a cholesterol transport defective CHO cell line isolated by Cadigan, Spillane, and Chang (17). This analysis identified six mutants that express an NPC-like phenotype in one complementation class, termed ced-1. One mutant (3-6) was identified in a separate, ced-2, complementation class (18).

In this study, biochemical analyses of ced-2 mutant 3-6 were performed to identify the cholesterol transport pathway(s) and responses that are affected by the mutation. Our results show that the 3-6 mutation causes defective mobilization of cholesterol from the plasma membrane to the endoplasmic reticulum. The characterization of this mutant line will facilitate the identification of gene products required for this transport pathway. Additionally, this mutant line will be a valuable tool for elucidating other cellular cholesterol transport pathways and homeostatic responses that do not require the movement of cholesterol from the plasma membrane into the cell.

MATERIALS AND METHODS

Materials

[1,2,6,7-^{3}H]cholesteryl linoleate (CL) (91.5 Ci/mmol), [1,2-^{3}H]cholesterol (51.0 Ci/mmol), and [^{3}H]acetic acid, sodium salt (135.4 mCi/mmol), were purchased from DuPont-New England Nuclear (Boston, MA). Mevinolin was a generous gift from A. Alberts, Merck Research Laboratory (Rahway, NJ). 25-Hydroxycholesterol (25-HC), cholesterol, and cholesterol sulfate from Steraloids (Wilton, NH) were added to medium in ethanolic solutions; amphotericin B was dissolved in dimethyl sulfoxide. Solvents were high-pressure liquid chromatography grade and purchased from Fisher Scientific (Pittsburgh, PA). Newborn calf serum and all other reagents were from Sigma Chemical Co. (St. Louis, MO) or obtained as previously described (13).

Preparation of LDL, lipoprotein-deficient serum, media, and buffers

LDL was prepared by ultracentrifugation (19). Lipoprotein-deficient serum was prepared from newborn calf serum omitting the thrombin incubation (19). [^{3}H]CL-LDL was prepared with an average specific activity of 7500 cpm/nmol of total CL (20).

The following media were prepared: Ham's medium [Ham's F-12 medium containing 2 mM glutamine, 100 units/ml penicillin, 100 μg/ml streptomycin, and 20 mM HEPES, pH 7.1]; H-5%NCS [Ham's medium containing 5% (v/v) newborn calf serum]; H-5%NCLPDS [Ham's medium containing 5% (v/v) lipoprotein-deficient calf serum]; H-1%NCLPDS [Ham's medium containing 1% (v/v) lipoprotein-deficient calf serum]; H-5%NCLPDS/mevinolin (H-5%NCLPDS containing 20 μM mevinolin and 0.5 mM mevalonate); and MEM-BSA [minimal essential medium containing 10 mM HEPES, pH 7.0, and 0.2% bovine serum albumin (BSA)].

The following buffers were prepared: TBS (150 mM NaCl, 50 mM Tris-chloride, pH 7.4); TBS-BSA (TBS containing 2 mg/ml BSA); SEH (250 mM sucrose, 1 mM EDTA, and 20 mM HEPES, pH 7.3) and PBS (2.7 mM KCl, 1.5 mM KH_2PO_4, 137 mM NaCl, 8.1 mM Na_2HPO_4, pH 7.3).

Cultured cells

Parental and mutant CHO-K1 cells were grown as monolayers in a humidified incubator (5% CO_2) at 37°C in H-5%NCS. On day 0 of each experiment, monolayer stock flasks were trypsinized, and cells were seeded as indicated in the individual experiment.

Protein determination

Cell protein was determined by dissolving cell monolayers in 0.1 N NaOH. Aliquots were removed and protein was determined by the method of Lowry et al. (21) using BSA as a standard.

Movement of endogenously synthesized sterols to the plasma membrane

Cells were seeded, grown, and pulse-labeled as described in the figure legend. Small unilamellar vesicles were prepared with a cholesterol/phosphatidylcholine molar ratio of 0.7, as previously described (15). Media and cells were harvested at staggered times, and medium and cellular [^{3}H]sterol were quantified as described (15), except that thin-layer chromatography (TLC) separation of [^{3}H]sterol and [^{3}H]steryl ester was performed using heptane–ethyl ether 90:60. The endogenously labeled [^{3}H]sterols contained a mixture of [^{3}H]cholesterol and [^{3}H]desmosterol (22).

Percoll gradient fractionation of [^{3}H]CL-LDL-labeled cells

Cells were seeded, grown, and pulse-labeled as described in the figure legend. On day 4, monolayers were harvested, fractionated, and the fractions were assayed

for [^{3}H]cholesterol content as previously described (11). Lysosomes were localized in the gradient fraction by measuring N-acetyl-β-glucosaminidase activity and plasma membranes were localized using wheat germ agglutinin linked to horseradish peroxidase, exactly as described (15).

Filipin fluorescence microscopy

Cells were seeded on coverslips in 6-well plates at 15,000 cells per well in H-5%NCS. After 2 days, cells were washed with PBS, fixed in 3% (w/v) paraformaldehyde in PBS for 30 min, and washed again with PBS (23). Cells were incubated with filipin (Sigma) at 25 μg/ml in PBS, washed with PBS, and mounted in glycerol (23). Samples were viewed utilizing a Zeiss Axiovert fluorescence microscope.

Cell growth

Cells were seeded and grown as described in the figure legend. On day 5, cells were washed and the protein content of each well was determined (15). Cell growth is expressed as microgram of cell protein/well.

Sphingomyelinase, 25-hydroxycholesterol, and cholesterol stimulation of cholesterol esterification

Cells were grown, incubated with [^{3}H]cholesterol, and treated with either sphingomyelinase, 25-HC, or cholesterol as described in the figure legends. At time of harvest, cells were washed with TBS at 4°C once quickly, once for 7 min, and once quickly. Monolayers were extracted with hexane–isopropyl alcohol 3:2, and 54 μg of cholesterol and 28 μg of cholesteryl oleate were added as a chromatography carrier. The cell extracts were evaporated to dryness and free and esterified cholesterol were separated by TLC on silica gel 60 plates (Brinkman, Westbury, NY) developed in toluene–ethyl acetate 2:1. Radioactivity was measured by liquid scintillation counting using Ready Safe (Beckman, Fullerton, CA).

Phospholipid composition

Cells were grown as described in the table legend. On day 4, monolayers were washed with TBS, scraped, and pelleted by centrifugation (2000 *g*, 5 min, 4°C). Each pellet, which contained the cells from three 150-mm dishes, was resuspended in distilled water and the lipids were extracted following the method of Bligh and Dyer (24). The lower, lipid-containing layer was washed twice with pure upper phase (chloroform–methanol–water 15:175:180). Phospholipids were separated on glass-backed silica gel 60 plates using a two-dimensional TLC system (chloroform–methanol–glacial acetic acid 65:25:5 in the first dimension and chloroform–methanol–formic acid 65:25:5 in the second dimension (25)). Phospholipids were visualized using iodine vapor and identified by comparison to authentic lipid standards (Matreya, Inc., Pleasant Gap, PA). Using this TLC system, sphingomyelin resolved into two species. Lipid spots were scraped, digested in perchloric acid, and the phosphate content was determined using the described microassay (26). The content of each phospholipid species is expressed as a percentage of total phospholipid.

Cholesterol content

Cells were grown in various media as described in the table legend. On day 4, cells were washed with TBS and extracted with hexane–isopropyl alcohol 3:2. Stigmasterol was added as an internal standard. Lipid extracts from two dishes were pooled, washed once with water, and the upper lipid phase was divided equally into two tubes per pooled sample. Free cholesterol was quantified by gas–liquid chromatography using a 3% OV-17 on 80/100 Gas Chrom Q column (6 feet by 0.085 inch, internal diameter) (Alltech Associates, Inc., Deerfield, IL). The second lipid aliquot was saponified for determination of total cholesterol (27). The esterified cholesterol was calculated by subtracting free cholesterol from total cholesterol. Cholesterol content is reported as microgram cholesterol/mg protein.

Semliki Forest virus infection and membrane fusion

To assess the susceptibility of parental CHO and mutant 3-6 cells to Semliki Forest virus (SFV), cells were cultured on 12-mm coverslips and switched to H-5%NCLPDS 1–2 days before use. Infection assays were performed as previously described (28) by binding serial dilutions of virus in binding medium (bicarbonate-free RPMI containing 10 mM HEPES, pH 7.0, and 0.2% BSA) to the cells on ice for 1 h. The cells were then incubated 2 h at 37°C in MEM-BSA to permit infection. The medium was then changed to MEM-BSA plus 20 mM NH_4Cl to prevent endosome acidification and secondary infection, and the cultures were incubated overnight at 28°C. Infected cells were quantitated by immunofluorescent staining with an antibody to the SFV spike protein. Fusion assays (28) were performed by similar prebinding of cells with virus on ice. Cells were then treated for 1 min at 37°C with binding medium containing 20 mM NH_4Cl and 10 mM 2(N-morpholino)ethanesulfonic acid, adjusted to either pH 7.0 (control) or pH 5.5 to trigger low pH-dependent fusion with the plasma membrane. Cultures were then incubated overnight at 28°C in MEM-BSA with 20 mM NH_4Cl, and infection quantitated by immunostaining and fluorescence microscopy as above. Parallel coverslips were tested for amphotericin B resistance by incubating for 6–8 h with 175 μg/ml amphotericin B in H-5%NCLPDS. Parental CHO cells were lysed while mutant cells were highly resistant (data not shown).

Cholesterol oxidase treatment

Cells were grown and labeled with [^{3}H]cholesterol as described in the table legend. On day 4, cells were washed with TBS-BSA at 4°C three times for 5 min each, then twice quickly with PBS. Cells were treated with cholesterol oxidase according to one of two methods. Method 1: following the method of Porn and Slotte (29), cells were fixed at room temperature for 10 min in 1% glutaraldehyde in PBS, washed, then treated for 30 min at 37°C with 0.1 U/ml sphingomyelinase with or without 2 U/ml cholesterol oxidase (Beckman or Calbiochem) in Ham's medium. Method 2: following the method of Smart et al. (30), cells were treated for 1 h at 37°C with or without 0.5 U/ml cholesterol oxidase in Ham's medium. After treatment by either method, all cells were washed twice for 2 min each at 4°C with PBS. Monolayers were extracted with hexane–isopropyl alcohol 3:2, and 40 μg of cholesterol and 20 μg of cholest-4-en-3-one (Steraloids) were added as chromatography carriers. The cell extracts were evaporated to dryness and cholesterol and cholestenone were separated by TLC on silica gel 60 plates with hexane–ethyl ether–glacial acetic acid 65:15:1. Radioactivity was measured by liquid scintillation counting.

Amphotericin B killing

Cells were grown in various media as described in the figure legend. On day 4, cells were tested for amphotericin B resistance by incubating the monolayers for 6 h with 175 μg/ml of amphotericin B in H-1%NCLPDS. On day 5, cells were washed with TBS at 4°C once quickly, 3 times for 10 min each, and once quickly. The protein was determined using a no cell/standard curve 12-well plate as previously described (15). Amphotericin B survival of cells with LDL or cholesterol sulfate addition is expressed as a percentage of survival of cells with no additions.

Statistical analysis

Statistical comparisons were made using a standard two-tailed, unpaired Student's *t* test or Mann-Whitney test (GraphPad InStat t_m, GraphPad Software V2.02).

RESULTS

Previously, we utilized amphotericin B to isolate CHO cells with defects in the transport of LDL-cholesterol to the plasma membrane (11). Mutagenized CHO cells were incubated in medium containing mevinolin to inhibit endogenous cholesterol synthesis, and LDL, a source of exogenous cholesterol. Cells were then treated with amphotericin B, a polyene antibiotic that forms pores in cholesterol-rich membranes. Cells capable of transporting LDL-cholesterol to the plasma membrane are lysed and killed by amphotericin B, while cells expressing mutations in the cholesterol transport pathway survive amphotericin B treatment.

Among our collection of somatic cell mutants defective in cholesterol transport, six belong to the ced-1 complementation class and express a classical NPC phenotype. This class includes mutants 2-2 and 4-4. The hallmark of this class is defective LDL-stimulation of cholesterol esterification commensurate with lysosomal accumulation of LDL-derived cholesterol. One mutant, 3-6, belongs to a new complementation class, termed ced-2. The present analysis is focused on defining the cholesterol transport pathways that are affected by the 3-6 mutation.

Movement of endogenously synthesized sterol to the plasma membrane

The movement of newly synthesized sterols to the plasma membrane was assessed in parental and mutant CHO cells by pulse-labeling cells for 1 h with [^{3}H]acetate followed by chase incubations for various times. Sterol synthesis was equivalent in the three cell lines, and CHO, 3-6, and 4-4 cells contained 22.3, 18.7, and 23.8 cpm/μg of [^{3}H]sterols, respectively. The relative movement of endogenously synthesized [^{3}H]sterols to the plasma membrane was determined by quantifying the amount of [^{3}H]sterol that desorbed from the cells and appeared in the medium during chase incubations. Chase incubations were performed in media containing small unilamellar vesicles to provide an adequate trap for the desorbed sterols. Small unilamellar vesicles were prepared with a cholesterol/phosphatidylcholine ratio similar to that of plasma membranes in order to promote cholesterol exchange, rather than net cholesterol movement (15).

In CHO cells, we found a time-dependent appearance of newly synthesized [^{3}H]sterols in the medium, which was due to movement of sterol to the plasma membrane and desorption from the cell surface (**Fig. 1**). The transport and desorption of nascent [^{3}H]sterols was equivalent in CHO, 4-4, and 3-6 cells, which indicates that both mutant cell lines transport newly synthesized sterols to the plasma membrane with normal kinetics. At each time point, the difference between CHO and 3-6 cells was not statistically significant. This finding was observed in three experiments.

Intracellular movement of LDL-derived cholesterol

Ced-1 mutants 2-2 and 4-4 exhibit impaired movement of LDL-cholesterol from lysosomes to the plasma membrane that is characteristic of NPC cells (15). How-

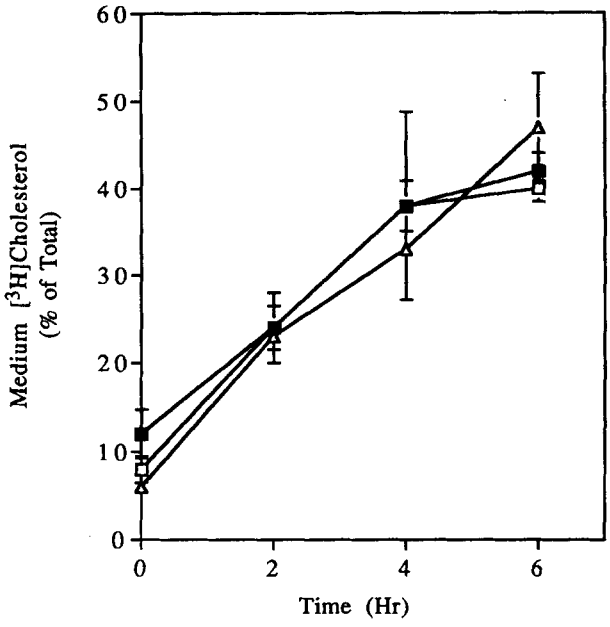

Fig. 1. Movement of synthesized cholesterol to the plasma membrane. CHO (■), 3-6 (□), and 4-4 (△) cells were seeded in 6-well plates at 20,000 cells/well in H-5%NCS. On day 1, cells were washed with 2 ml of EBSS and refed 1 ml of H-5%NCLPDS. On day 3, cells were refed 1 ml of H-5%NCLPDS. On day 4, cells were incubated with 30 μCi/ml [^{3}H]acetate for 1 h. Monolayers were then washed with EBSS and refed 1 ml of H-5%NCLPDS/mevinolin containing 25 μl small unilamellar vesicles (1 μmol of cholesterol and 1.45 μmol of L-α-phosphatidylcholine). The media were removed and cells were harvested at staggered times. Cellular [^{3}H]cholesterol and medium [^{3}H]cholesterol were determined as described under Materials and Methods. Medium [^{3}H]cholesterol is expressed as a percentage of the sum of cellular and medium cholesterol at each time point. Each data point represents the mean and standard deviation of triplicate cultures.

ever, our preliminary analysis of ced-2 mutant 3-6 indicated that the transport of LDL-[^{3}H]cholesterol from lysosomes to plasma membranes was normal.

To determine whether mutant 3-6 exhibits the lysosomal storage of LDL-cholesterol that is characteristic of ced-1 mutants, CHO and mutant cells were continuously labeled with [^{3}H]CL-LDL. Cells were homogenized and postnuclear supernatants were fractionated on Percoll density gradients to separate lysosomes, which are dense and fractionate to the bottom of the gradient, from other subcellular organelles. Ten fractions were obtained from each gradient, and the location of organelles was determined by measuring the distribution of marker enzyme activities (data not shown). In previous studies, we showed that a cytosolic marker enzyme appears in fraction 1, marker enzymes for the light membranes (ER, Golgi apparatus, and plasma membrane) co-localize in fractions 2–4, while a lysosomal marker appears in fractions 9–10 (15).

The distribution of LDL-derived [^{3}H]cholesterol in lysosomes and light membranes is shown in **Fig. 2.** In CHO cells, LDL-derived [^{3}H]cholesterol accumulated in lysosomes to approximately 700 pmol/fraction in 1.5 h and did not increase significantly for the remainder of the time course (panel A). In contrast to the plateau observed in the lysosomes, the appearance of LDL-derived [^{3}H]cholesterol in the light membranes increased throughout the time course (panel B). This indicates that the appearance of LDL-derived [^{3}H]cholesterol in lysosomes (receptor-mediated uptake and hydrolysis) is balanced by movement of the sterol from lysosomes to other cellular membranes.

As shown previously (11), the NPC-like ced-1 mutant 2-2 accumulated LDL-derived cholesterol in lysosomal fractions (panel A) and this accumulation did not plateau during the 6-h time course. The appearance of [^{3}H]cholesterol in the light membranes fractions was slower (panel B), indicating that LDL-derived cholesterol transport from the lysosomes to other cell membranes is impaired.

Similar to CHO cells, mutant 3-6 accumulated LDL-derived [^{3}H]cholesterol in lysosomes to approximately 700 pmol/fraction in 1.5 h, and this amount did not increase for the remainder of the time course (panel A). Although there was a slight lag in the appearance of LDL-derived cholesterol in the light membranes, the cholesterol level increased throughout the time course (panel B). This finding that, unlike the ced-1 class of mutants, mutant 3-6 did not exhibit lysosomal storage of LDL-derived cholesterol, was observed in three separate experiments.

Lysosomal storage of LDL-cholesterol was also investigated by filipin fluorescence microscopy. Filipin is a fluorescent polyene antibiotic that binds specifically to cholesterol and is used to detect cellular cholesterol pools (23). Mutant 3-6 cells incubated with LDL were indistinguishable from CHO cells, showing no lysosomal cholesterol accumulation (data not shown). Thus, our results with filipin fluorescence microscopy confirmed the subcellular fractionation results.

LDL and cholesterol sulfate-dependent cell growth

Our experiments thus far demonstrated that cholesterol transport pathways towards the plasma membrane are normal. The next set of experiments was designed to determine whether the cholesterol that arrived at the plasma membrane was available for cellular growth.

Mammalian cells require an exogenous source of cholesterol for growth when cultured in the presence of mevinolin, an inhibitor of mevalonate synthesis, and thus, cholesterol biosynthesis (31, 32). We tested the ability of LDL-derived cholesterol to reverse mevinolin-inhibited cell growth in parental and mutant CHO cells (**Fig. 3,** panel A). Cell monolayers were grown for 5 days

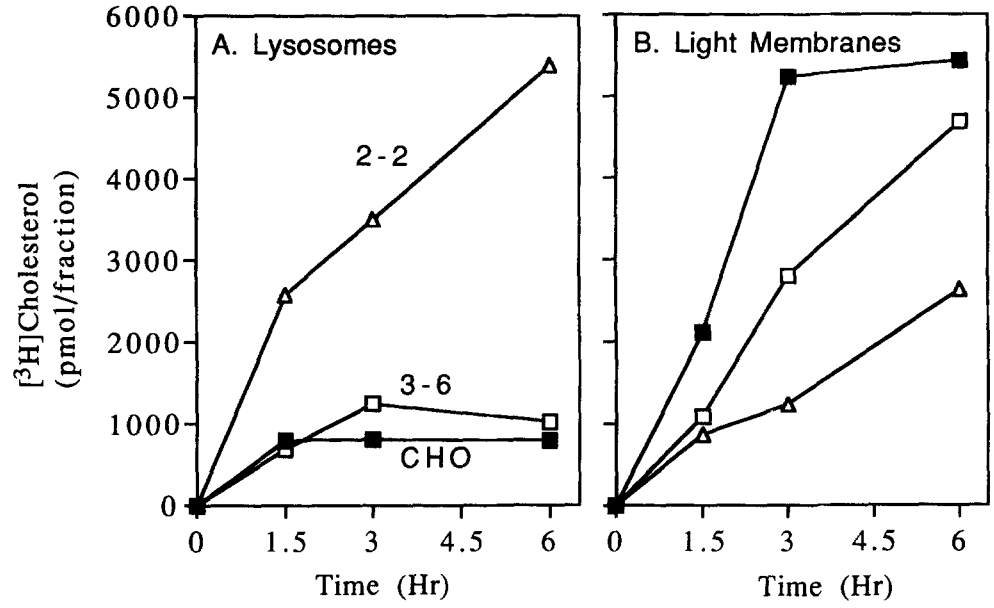

Fig. 2. [^{3}H]cholesterol content in lysosomal (panel A) and light membrane (panel B) Percoll gradient fractions from continuously labeled cells. CHO (■), 3-6 (□), and 2-2 (△) cells were seeded in 150-mm dishes at 150,000 cells/dish in H-5%NCS. On day 1, cells were washed with 10 ml of EBSS and refed 20 ml of H-5%NCLPDS. On day 3, cells were refed 17 ml of H-5%NCLPDS. On day 4, cells were pulsed at staggered times with [^{3}H]CL-LDL (8 μg/ml). All dishes were harvested at the same time. Percoll gradient fractionation of postnuclear supernatants was carried out, and the [^{3}H]cholesterol content of gradient fractions was determined as described under Materials and Methods. The [^{3}H]cholesterol content of gradient fractions with high N-acetyl-B-glucosaminidase activity (fractions 9 and 10) were summed (Lysosomes, panel A). The [^{3}H]cholesterol content of gradient fractions with high WGA-HRP activity (fractions 2–4) were summed (Light Membranes, panel B). The data points at each time represent the sum of [^{3}H]cholesterol in the designated fractions from one gradient, expressed as pmol/fraction.

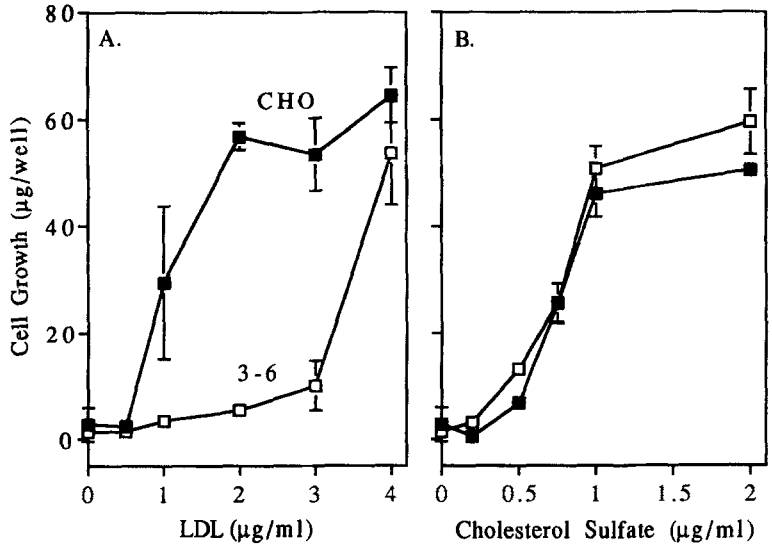

Fig. 3. LDL-, cholesterol-, and cholesterol sulfate-dependent growth of CHO and mutant cells. CHO (■) and 3-6 (□) cells were seeded in 12-well plates at 5000 cells/well in 2 ml of H-5%NCLPDS. After 6 h, cells were washed with EBSS and refed 1 ml of H-5%NCLPDS/mevinolin containing no additions or various amounts of LDL, cholesterol, or cholesterol sulfate. On day 5, monolayers were washed and the protein content of each well was measured as described in Materials and Methods. Cell growth values are the mean and standard deviations of quadruplicate cultures.

in H-5%NCLPDS/mevinolin containing varying concentrations of LDL, after which the protein content of the wells was measured as an indicator of cell growth.

The growth of CHO cells cultured in H-5%NCLPDS/mevinolin (without a source of cholesterol) was inhibited and the wells contained 3 μg/well of protein. The addition of LDL to mevinolin-inhibited cells increased cell growth in a concentration-dependent manner, such that normal cells cultured with 2 μg/ml LDL increased their protein content to 55 μg/well. The protein content in wells of 3-6 cells grown in H-5%NCLPDS/mevinolin was 1 μg/well. Although the addition of LDL-cholesterol to the medium reversed mevinolin-inhibited growth of mutant 3-6, a higher concentration of LDL was needed to stimulate growth relative to CHO cells. At low LDL concentrations (1–3 μg/well), the differences observed between CHO and 3-6 cells were significant ($P < 0.05$).

Cultured mammalian cells also grow in the presence of mevinolin when the media is supplemented with cholesterol sulfate, which is hydrolyzed by an ER steroid sulfatase to provide the cell with free cholesterol (33, 34). We observed that cholesterol sulfate restored growth in mutant 3-6 equally or slightly better than in parental CHO cells (panel B). These LDL- and cholesterol sulfate-dependent growth results were observed in three separate experiments.

Cells cultured in H-5%NCLPDS have endogenously synthesized cholesterol available for growth, and the protein content in wells of CHO cells cultured in H-5%NCLPDS was 56 μg/well. However, the protein content in wells of mutant 3-6 cultured in H-5%NCLPDS was 2 μg/well. Thus, 3-6 cells do not efficiently utilize endogenously synthesized cholesterol for growth despite our findings that they have normal levels of 3-hydroxy-3-methylglutaryl (HMG)-CoA reductase activity (18) and synthesize [^{3}H]sterol from [^{3}H]acetate at 84% of parental CHO levels.

The above results demonstrate that 3-6 cells transport LDL-derived and endogenously synthesized cholesterol to the plasma membrane; however, that cholesterol is inefficiently used for cell growth. Furthermore, we previously showed that 3-6 cells are unable to stimulate cholesterol esterification or suppress HMG-CoA reductase as normal in response to LDL (18). Together, these findings suggest that either cholesterol movement or signaling to the cell interior may be defective.

Sphingomyelinase stimulation of cholesterol esterification

To evaluate movement of cholesterol from the plasma membrane to the ER, we utilized the method of Slotte and Bierman (3) and Porn and Slotte (29) to digest plasma membrane cholesterol with a phospholipase C-type sphingomyelinase. Sphingomyelin digestion causes both a redistribution of cholesterol within the plasma membrane and a flow of 5–10% of the plasma membrane cholesterol to the ER, where it is metabolized to cholesteryl ester by acyl-CoA:cholesterol acyltransferase (ACAT) (35).

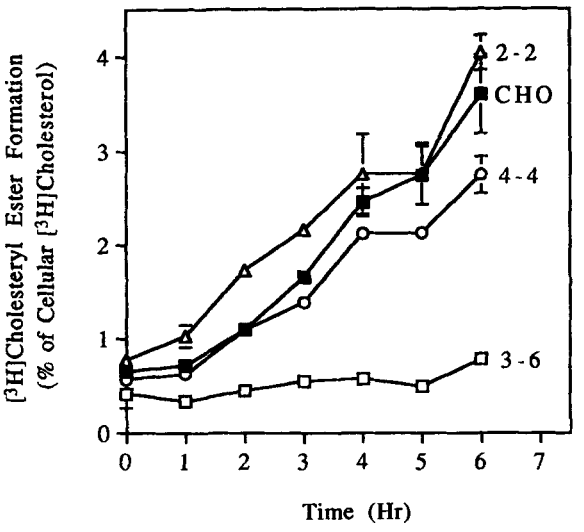

Fig. 4. Sphingomyelinase stimulation of cholesterol esterification. CHO (■), 3-6 (□) 4-4 (○), and 2-2 (△) cells were seeded in 6-well plates at 10,000 cells/well in H-5%NCLPDS. On day 1, cells were washed with EBSS and refed 1 ml of H-5%NCLPDS. On day 2, the cells were refed 1 ml of H-5%NCLPDS containing 1 μCi/ml [^{3}H]cholesterol. On day 3, cells were washed with EBSS and refed 1 ml of H-5%NCLPDS. After 30 min, cells were washed with 2 ml of EBSS and refed 1 ml of Ham's medium. Additions of 100 mU/ml sphingomyelinase were made at staggered times. All dishes were harvested at the same time as described under Materials and Methods. The [^{3}H]cholesteryl ester formed is expressed as a percentage of the total cellular [^{3}H]cholesterol and [^{3}H]cholesteryl ester. Each data point represents the average of two wells, and the observed ranges are shown. For some values, the range is obscured by the symbol.

A time course of sphingomyelinase stimulation of cholesterol esterification was performed in parental and mutant cells (**Fig. 4**). Cellular cholesterol pools were labeled by incubating the cells with [^{3}H]cholesterol for 15 h, after which cells had incorporated from 120,000–155,000 cpm/well. Cells were treated for 0–6 h with sphingomyelinase and the amount of free [^{3}H]cholesterol and [^{3}H]cholesteryl ester at each time point was determined.

In parental CHO cells, sphingomyelinase treatment led to a time-dependent increase in cellular cholesteryl ester content, such that by 6 h 3.7% of cellular cholesterol was esterified. Similar rates of cholesterol esterification were measured when ced-1 mutants 2-2 and 4-4 were treated with sphingomyelinase. In ced-2 mutant 3-6, however, cholesteryl ester levels remained unchanged, even after 6 h of sphingomyelinase treatment. Therefore, we conclude that the 3-6 mutation affects

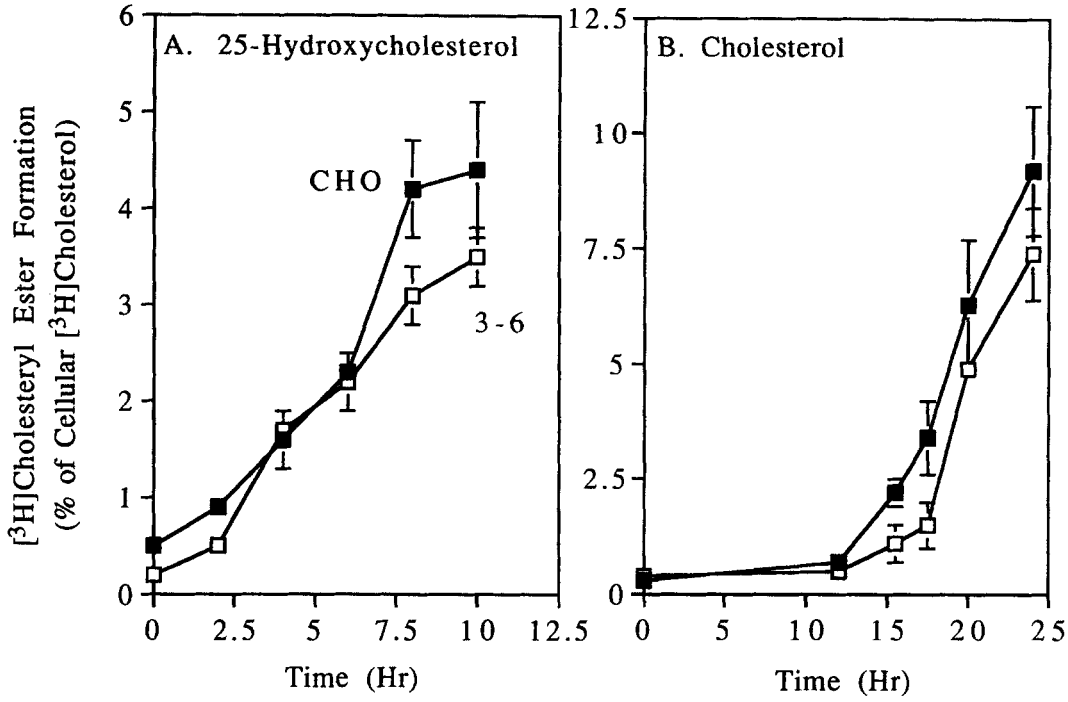

Fig. 5. 25-Hydroxycholesterol and cholesterol stimulation of cholesterol esterification. CHO (■) and 3-6 (□) cells were seeded in 6-well plates at 10,000 cells/well in H-5%NCS. On day 1, cells were washed with EBSS and refed 1 ml of H-5%NCLPDS containing 1 μCi/ml [^{3}H]cholesterol. For the 25-HC treatment (panel A), on day 2, cells were washed with 2 ml of EBSS and refed 1 ml of H-5%NCLPDS/mevinolin. On day 3, additions of 1 μg/ml 25-HC were made at staggered times. For the cholesterol treatment (panel B), on day 2, cells were washed with 2 ml of EBSS and refed 1 ml of H-5%NCLPDS/mevinolin. Additions of 20 μg/ml of cholesterol were made at staggered times. On day 3, all cells were harvested at the same time as described under Materials and Methods. The [^{3}H]cholesteryl ester formed is expressed as a percentage of the total cellular [^{3}H]cholesterol and [^{3}H]cholesteryl ester. Each data point represents the mean and standard deviation of triplicate cultures.

the mobilization of cholesterol from the cell surface to the ER. These results were observed in five separate experiments.

One explanation for the above result may be ineffective sphingomyelin degradation when 3-6 cells are treated with sphingomyelinase. However, we determined that sphingomyelinase treatment for 5 h digested 71.5% and 72.6% of cellular sphingomyelin in CHO and 3-6 cells, respectively. Hence, the lack of cholesteryl ester formation in mutant 3-6 after sphingomyelinase treatment is not due to impaired sphingomyelin digestion.

Another possible explanation for the above result is that mutant 3-6 is defective in ACAT activity. In cultured cells, ACAT is stimulated when cells are incubated with oxygenated sterols, such as 25-HC (36). **Figure 5A** shows the ability of 1 μg/ml 25-HC to stimulate cellular [^{3}H]cholesterol esterification in CHO and 3-6 cells. Formation of [^{3}H]cholesteryl esters is equivalent in both cell types at early times, although there is greater cholesterol esterification in CHO cells by 8–10 h. Similarly, we found that [^{3}H]cholesterol esterification could be stimulated in both cell lines by the addition of cholesterol, which serves as both an ACAT activator and substrate (37) (Fig. 5B). At most time points, the difference between CHO and 3-6 cells was not statistically significant. These results indicate that, once ACAT is activated, delivery of cellular cholesterol to the enzyme in the ER is not affected by the 3-6 mutation. The 25-HC results were observed in six experiments, and the cholesterol results were observed in two experiments.

In wild-type CHO cells, the cholesterol that is esterified when ACAT is activated is likely to be a mix of plasma membrane cholesterol and cholesterol from intracellular pools. However, when ACAT is activated by 25-HC in mutant 3-6, our sphingomyelinase data indicate that the plasma membrane pool is unavailable for transport to the ER. Our hypothesis is that, in 3-6 cells, more intracellular cholesterol must be mobilized to ACAT under these conditions. Consistent with this idea are our results with pharmacological inhibitors of plasma membrane to ER transport in CHO cells. One drug that inhibits this pathway is U18666A (35). When Underwood et al. (38) stimulated cholesterol movement from the plasma membrane to ACAT by sphingomyelinase treatment of CHO cells, U18666A inhibited

transport with an IC_{50} of 0.5 μM. We find that 25-HC stimulation of cholesterol esterification is not significantly inhibited at U18666A concentrations up to 50 μM (data not shown). Thus, concentrations of U18666A that completely block the transport of cholesterol from the plasma membrane to ER have no effect on 25-HC stimulation of cholesterol esterification. These findings suggest that when the plasma membrane to ER pathway is inhibited, mobilization of an intracellular cholesterol pool to ACAT must be increased.

Cellular content of phospholipids

The above results demonstrating that cholesterol movement to the cell interior is affected by the 3-6 mutation focused our analysis on the plasma membrane. First, we examined the total cellular content of phospholipids, paying particular attention to the sphingomyelin content. As 90% of cellular sphingomyelin is localized at the plasma membrane (39), it is likely to play an important role in the cholesterol distribution.

The cellular content of the major phospholipid species was determined by extracting the lipids, separating them by two-dimensional TLC, and quantifying the percentage of phospholipid in each of the major classes. The analysis shown in **Table 1** revealed no major differences in phospholipid content between CHO, 4-4, and 3-6 cells indicating that the 3-6 phenotype was not due to a major difference in phospholipid content. Two species of sphingomyelin were detected, most likely due to differences in acyl chain length. Equivalent amounts of both sphingomyelin species were observed in all three cell lines. These findings were observed in two experiments.

Cellular content and distribution of cholesterol

The cholesterol content and distribution within the cell was assessed using three approaches. First, cellular levels of free and esterified cholesterol were measured by gas–liquid chromatography and normalized to cell protein **(Table 2).** In two experiments, CHO and 3-6 cells grown in H-5%NCS had identical cholesterol contents. After 4 days of growth in H-5%NCLPDS, the free cholesterol content in 3-6 cells was 76% of control cells.

As a second assay of the distribution and accessibility of cholesterol in the plasma membrane, we tested the infection and fusion of CHO and 3-6 cells with SFV. This enveloped virus infects cells by endocytic uptake followed by low pH-triggered membrane fusion within the endosome (40). SFV fusion requires cholesterol or a 3β-hydroxysterol in the target membrane (41), and fusion is inhibited by cholesterol depletion of either BHK cells or a mosquito cell line (42). Virus susceptibility of CHO and 3-6 cells was tested by an infectious center assay that detects primary infection (28, 43). As shown in **Table 3,** both CHO and 3-6 cells were comparably infected by SFV in three experiments. Previous work showed that cholesterol-depleted cells that are refractory to SFV infection are more susceptible to inhibition in a direct membrane fusion assay (28). SFV fusion with normal and mutant 3-6 cells was therefore tested by binding serial dilutions of virus to the cells in the cold, treating briefly at low pH to trigger fusion, and culturing cells in the presence of 20 mM NH_4Cl to allow virus protein expression in the absence of secondary infection. Under these conditions, SFV infection occurs due to the direct fusion of the virus membrane with the target membrane (28, 44). As shown in Table 3, both CHO and 3-6 cells were efficiently infected by plasma membrane fusion. Similar to our previous results, such fusion gave titers only about 10-fold lower than those obtained by the normal endocytic route (28). Taken together, these results indicate that the concentration and accessibility of cholesterol in the 3-6 mutant were sufficient to support SFV membrane fusion. The data shown in the figure are the mean and standard deviation of three experiments.

A third method to assess the percentage of cholesterol at the plasma membrane was cholesterol oxidase treatment of [^{3}H]cholesterol-labeled cells. Cells were labeled with [^{3}H]cholesterol for 16 h, then glutaraldehyde-fixed and subjected to oxidase treatment according to the method of Porn and Slotte (29) (Method 1). [^{3}H]cholesterol converted to [^{3}H]cholestenone was quantified. **Table 4** shows that in the absence of cholesterol oxidase treatment, 0.3% of the radiolabel comigrated with cholestenone in all cell lines, most likely due to an impurity present in the labeled cholesterol. In CHO and 4-4 cells, 63.4% and 68.1% of [^{3}H]cholesterol was susceptible to oxidation, respectively. This result is consistent with Warnock et al. (2), who found that CHO plasma membranes contain 64% of cellular

TABLE 1. Cellular content of phospholipids

Phospholipid	Cell Line		
	CHO	4-4	3-6
	% of total phospholipid		
Sphingomyelin	11.6 ± 1.4	12.7 ± 0.5	12.3 ± 1.4
	4.4 ± 0.8	4.3 ± 0.5	4.1 ± 0.4
PtdIns	4.7 ± 1.0	4.4 ± 0.8	4.4 ± 1.0
PtdCho	55.0 ± 2.3	51.4 ± 1.9	48.0 ± 4.5
PtdEtn	19.4 ± 3.2	21.7 ± 3.1	24.2 ± 2.9
PtdA	3.0 ± 0.4	2.3 ± 0.7	2.3 ± 0.7

All cells were seeded in 150-mm dishes at 350,000 cells/dish in H-5%NCS. On day 2, monolayers were refed H-5%NCLPDS. On day 4, cells were harvested, cellular lipids were extracted and quantified as described under Materials and Methods. Phospholipid content is expressed as a percentage of total phospholipid and represents the mean and standard deviation of quadruplicate samples.

TABLE 2. Cellular levels of free and esterified cholesterol

Cell Line	Medium	Cholesterol		
		Total	Free	Esterified
		μg/mg protein		
Experiment 1				
CHO	LPDS	11	9.8	1.2
	NCS	26.2	18.1	8.1
3-6	LPDS	7.9	7.4	0.5
	NCS	22.5	17.0	5.5
Experiment 2				
CHO	LPDS	10.1	9.9	0.2
	NCS	15.5	12.2	3.4
3-6	LPDS	7.0	7.5	0.0
	NCS	19.5	14.5	4.9

Cells were seeded in 150-mm dishes at 300,000 cells/dish in H-5%NCLPDS. On day 2, the cells were refed H-5%NCS or H-5%NCLPDS. On day 4, the cells were harvested as described under Materials and Methods. Each data point represents the average of duplicate samples.

cholesterol. Mutant 3-6 contained 53.8% of cellular [^{3}H]cholesterol in a cholesterol oxidase-sensitive pool, which is 15% lower than control values and significantly different from parental CHO cells ($P < 0.05$) in this experiment. The difference was seen in a second experiment, although the difference was not significant in that experiment.

To examine the cholesterol oxidase-sensitive plasma membrane cholesterol pool further, [^{3}H]cholesterol-labeled cells were oxidase-treated according to the method of Smart et al. (30) (Method 2). By this method, cells are not fixed prior to oxidation. Smart et al. (30) showed that the pool of oxidase-sensitive cholesterol in living cells is in the caveolae, a membrane specialization involved in potocytosis. If 3-6 cells contain modified microdomain structures within the plasma membrane, altered oxidase-sensitive pools might be found. Table 4 shows that in the absence of cholesterol oxidase treatment, 0.3–0.4% of the radiolabel co-migrated with cholestenone. Oxidase treatment of living CHO cells converted 6.3% of cellular [^{3}H]cholesterol to [^{3}H]cholestenone, which is consistent with the 5–7% conversion in human fibroblasts reported by Smart et al. (30). Mutants 3-6 and 4-4 had 4.9% and 5.0%, respectively, of their cholesterol in an oxidase-susceptible pool. In both this and a second experiment, there was no significant difference between parental and mutant CHO cells. Therefore, we believe CHO and 3-6 cells have similar cholesterol oxidase-susceptible pool sizes.

TABLE 3. SFV infection and membrane fusion

Cell Line	Titer from Infection[a]	Titer from pH 5.5 Fusion[b]
	ic/ml	*ic/ml*
CHO	$3.5 \times 10^9 \pm 0.68 \times 10^9$	$1.7 \times 10^8 \pm 0.31 \times 10^8$
3-6	$1.7 \times 10^9 \pm 1.1 \times 10^9$	$4.1 \times 10^8 \pm 1.9 \times 10^8$

Cells were grown as described under Materials and Methods. Data shown are the means ± standard deviation of three experiments.

[a]For infection studies, serial dilutions of an SFV stock were bound to cells in the cold; the cells were treated for 1 h at 37°C to permit infection, and then incubated overnight in medium containing 20 mM NH_4Cl to permit expression of virus proteins. Virus spike protein-expressing cells were quantitated by immunofluorescence, and titers are expressed as infected cells/ml (ic/ml).

[b]For fusion studies, serial dilutions of an SFV stock were bound to cells in the cold; the cells were treated for 1 min at 37°C with pH 5.5 medium or pH 7.0 medium containing 20 mM NH_4Cl. Cells were then incubated overnight in medium containing 20 mM NH_4Cl to permit expression of virus proteins. Virus spike protein-expressing cells were quantitated by immunofluorescence, and titers are expressed as infected cells/ml (ic/ml). Titers resulting from pH 7 treatment were, on average, ~10% of those resulting from pH 5.5 treatment.

Amphotericin B-mediated cell killing

As mutant 3-6 exhibited normal movement of endogenously synthesized and LDL-derived cholesterol to the plasma membrane, 3-6 cells should be killed by the action of amphotericin B. Amphotericin B intercalates into sterol-rich plasma membranes, forming aqueous pores that cause cell lysis (45–47). Our original mutant selection protocol was designed to isolate cells that were amphotericin B-resistant after incubation with 9 μg/ml LDL, due to impaired transport of LDL-cholesterol to the plasma membrane. The NPC-like ced-1 mutants and the ced-2 mutant 3-6 all exhibited amphotericin B resistance after incubation with LDL (11).

Figure 6 illustrates LDL (panel A) and cholesterol sulfate-dependent (panel B) amphotericin B killing of CHO, 3-6, and 4-4 cells. Cells were preincubated for 24 h in various media with the indicated additions of LDL or cholesterol sulfate and then treated for 6 h with amphotericin B. The protein content of the wells was measured as an indicator of cell survival.

In the presence of mevinolin, endogenous cholesterol synthesis is inhibited and all three cell types were

TABLE 4. Quantification of cholesterol oxidase-sensitive pools of cholesterol

	[^{3}H]Cholestenone			
	Method 1		Method 2	
Cell Line	−ChOx	+ChOx	−ChOx	+ChOx
	% of [^{3}H]cholesterol			
CHO	0.3 ± 0	63.4 ± 2.8	0.3 ± 0.1	6.3 ± 0.9
3-6	0.3 ± 0	53.8 ± 1.6	0.3 ± 0	4.9 ± 0.3
4-4	0.3 ± 0	68.1 ± 0.8	0.4 ± 0.1	5.0 ± 1.1

All cells were seeded in 6-well plates at 25,000 cells per well in H-5%NCS. On day 1, monolayers were washed with EBSS and refed H-5%NCLPDS. On day 3, cells were refed 1 ml of H-5%NCLPDS containing 5 μCi of [^{3}H]cholesterol. After 16 h, cells were washed and cholesterol oxidase (ChOx)-treated according to the methods of Porn and Slotte (29) (Method 1) or Smart et al. (30) (Method 2), as described under Materials and Methods. Each data point represents the mean and standard deviation of triplicate samples.

amphotericin B resistant. In CHO cells, the addition of small amounts of LDL resulted in amphotericin B sensitivity and with 9 μg/ml of LDL, only 15% of the cells survived. Mutant 4-4 exhibited survival with all concentrations of LDL, and 55% of the cells survived with 9 μg/ml of LDL. Mutant 3-6 demonstrated resistance to amphotericin B at concentrations of LDL up to 9 μg/ml, at which level 75% of the cells survived. Thus, despite the fact that LDL cholesterol readily exits the lysosome and arrives at the plasma membrane (18), the 3-6 mutation results in reduced amphotericin B killing of the cells. CHO and 4-4 cells preincubated in media without mevinolin were sensitive to amphotericin B due to movement of endogenously synthesized cholesterol to the plasma membrane; however, mutant 3-6 showed amphotericin B resistance despite ongoing cholesterol synthesis and transport to the plasma membrane (data not shown).

Another source of cholesterol is cholesterol sulfate, which must be hydrolyzed by an ER steroid sulfatase to provide the cell with free cholesterol (33, 34). The addition of increasing amounts of cholesterol sulfate (panel

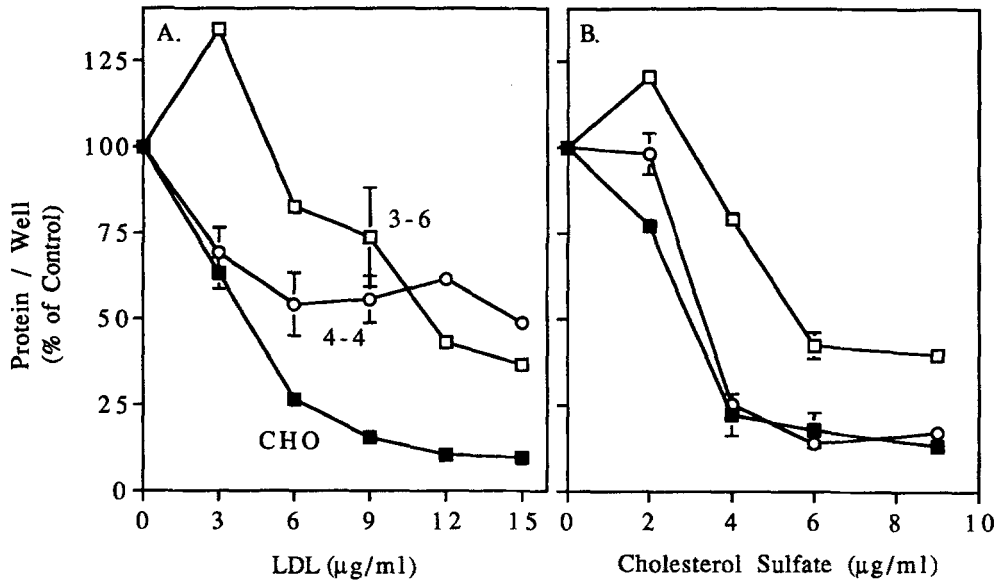

Fig. 6. LDL- and cholesterol sulfate-dependent amphotericin B killing of normal and mutant CHO cells. CHO (■), 3-6 (□), and 4-4 (○) cells were seeded in 12-well plates at 10,000 cells/well in H-5%NCS. On day 2, cells were washed with EBSS and refed 1 ml H-5%NCLPDS. On day 3, monolayers received 1 ml of H-5%NCLPDS/mevinolin and the indicated additions of LDL or cholesterol sulfate were made. After 24 h, cells received 1 ml of H-1%NCLPDS containing 175 μg/ml of amphotericin B. After 6 h, cells were washed with EBSS and refed 1 ml of H-5%NCS. On day 5, cells were washed and the cell protein content of each well was measured as described under Materials and Methods. The protein/well is expressed as a percentage of the protein value in wells incubated without LDL or cholesterol sulfate. Each data point represents the average of two wells, and the observed ranges are shown. For some values, the range is obscured by the symbol.

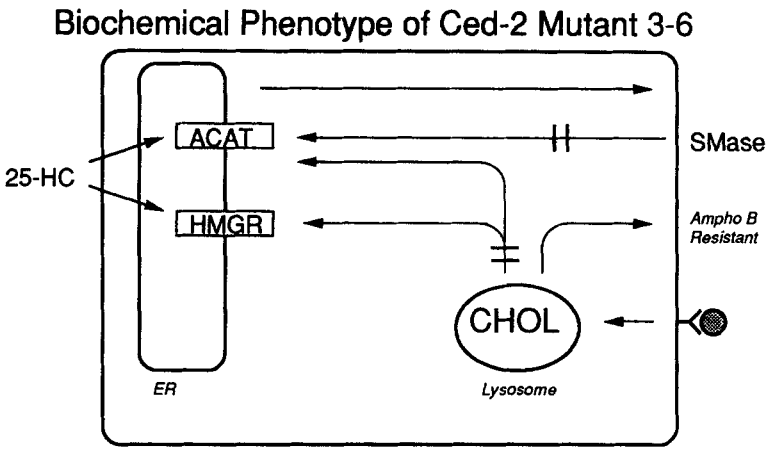

Fig. 7. Intracellular cholesterol transport and regulation in mutant 3-6. The internalization and movement of LDL to the lysosome is normal. The movement of cholesterol both from the ER and through the lysosomes to the plasma membrane is normal as well. Cholesterol transport from the plasma membrane to ACAT in the ER is defective. Additionally, the activation of ACAT and suppression of HMG-CoA reductase by LDL-cholesterol is impaired, although these homeostatic responses are normal in response to 25-HC.

B) correlated with increasing sensitivity to amphotericin B in all three cell lines; however, mutant 3-6 was less sensitive than CHO or 4-4 cells. Therefore, mutant 3-6 is relatively amphotericin B resistant when provided with either lipoprotein or non-lipoprotein-derived cholesterol, or with endogenously synthesized cholesterol. These results were observed in three separate experiments.

DISCUSSION

Two complementation classes of cholesterol transport mutants have been defined by our studies (18). The ced-1 class is characterized by expression of the classical NPC biochemical phenotype, exhibiting lysosomal storage of LDL-cholesterol and impaired transport of cholesterol from lysosomes to other cellular membranes (11). The transport deficiency is combined with abnormal LDL-mediated regulation of cellular cholesterol homeostasis. The ced-2 mutant 3-6 exhibits many of the ced-1 characteristics, such as defective LDL-stimulation of cholesterol esterification and impaired LDL suppression of HMG-CoA reductase (18); however, mutant 3-6 shows normal movement of cholesterol to the plasma membrane.

In this study, biochemical analysis of mutant 3-6 revealed three critical features (**Fig. 7**). The primary finding is that the mutation affects only one transport pathway, the movement of cellular cholesterol to ACAT in the ER. Additionally, 3-6 cells are unable to use endogenously synthesized sterol or LDL-cholesterol for growth as effectively as CHO cells. Finally, although trafficking of cholesterol to the plasma membrane is normal, the cells are resistant to amphotericin B. Based on the transport results as well as the other phenotypic characteristics of the cell line, our hypothesis is that the plasma membrane cholesterol domain structure is altered in 3-6 cells, which results in defective transport and regulation.

The first key feature of the 3-6 mutation is that it affects only one transport pathway, the movement of plasma membrane cholesterol to ACAT in the cell interior upon treatment of the cells with sphingomyelinase. Cholesterol transport pathways towards the plasma membrane are normal in the 3-6 mutant. Subcellular fractionation of [^{3}H-CL]LDL-labeled 3-6 cells and filipin fluorescence microscopy confirmed that movement of LDL-cholesterol through the lysosome to other cell membranes is normal. These data support our previous finding that LDL-cholesterol moves to the plasma membrane and desorbs to extracellular acceptors almost as efficiently in 3-6 as in CHO cells (18). Normal movement of endogenously synthesized cholesterol from the ER to the plasma membrane suggests that transport to the cell surface does not depend upon a functional return transport system.

While sphingomyelinase treatment does not stimulate mobilization of cellular cholesterol to ACAT, cellular cholesterol can be mobilized to the enzyme when it is directly activated by 25-HC. A portion of this cholesterol may originate from the plasma membrane; however, much of it must be mobilized from intracellular stores, which under our culture conditions account for approximately 30% of wild-type CHO cellular cholesterol.

The second key point is that mutant 3-6 does not utilize endogenously synthesized sterol or low levels of LDL-cholesterol for growth as effectively as CHO cells, although utilization of cholesterol sulfate is normal. Little is known about which cholesterol transport pathways are necessary for growth, but the results imply that merely filling the plasma membrane pool is not sufficient. Instead, cholesterol movement or signaling through the plasma membrane to the cell interior may

be required. Cholesterol sulfate added directly to the medium is metabolized in the ER and delivered to a pool that is available for growth, while nascent and LDL-cholesterol does not reach this pool.

The third important feature of the 3-6 mutant is that while trafficking of cholesterol to the plasma membrane is normal, 3-6 cells are amphotericin B-resistant when supplied with endogenously synthesized cholesterol, LDL, or cholesterol sulfate. These results were surprising because the amphotericin B selection protocol was designed to isolate cells with low plasma membrane cholesterol content due to defects in LDL-cholesterol transport to the cell surface.

Resistance to amphotericin B could be caused by reduction of cellular cholesterol content to 50% of control levels (48, 49). However, several tests have been performed to eliminate that possibility. Analysis of cholesterol and cholesteryl ester mass showed that CHO and 3-6 cells have identical cholesterol contents when grown in H-5%NCS. The mutant 3-6 cholesterol content falls to 76% of control levels after 4 days of growth in H-5%NCLPDS, yet they are amphotericin B-resistant after 2 days of growth in the lipoprotein-deficient serum. In addition, studies of SFV infection and fusion with CHO and 3-6 cells indicate comparable efficiency of virus–membrane fusion. In comparison, we have shown that cholesterol depletion of BHK cells to 30% of control levels strongly inhibits SFV plasma membrane fusion (42). In vitro studies of SFV fusion with liposomes demonstrated that fusion is maximal at a cholesterol/phospholipid ratio of 1:2, and the threshold cholesterol concentration for fusion is a ratio of 1:5 (50). The ability of 3-6 cells to support efficient SFV infection and fusion while remaining resistant to amphotericin B could be due to a difference in cholesterol concentration requirements. Alternatively, the results may point to a difference in sterol structure or accessibility requirements. While both SFV fusion (41) and amphotericin B lysis (46) require the sterol 3β-hydroxy group, other requirements for sterol structure or packing in the membrane may differ between the two probes. Although the reason for the difference between 3–6's susceptibility to SFV and amphotericin B is as yet unclear, our SFV studies provide additional evidence for the presence of cholesterol in the 3–6 plasma membrane. Therefore, we conclude that resistance of mutant 3–6 to amphotericin B treatment is primarily a result of altered cholesterol organization, rather than cholesterol content, in the plasma membrane.

In addition to affecting mobilization of cholesterol from the cell surface to the ER, cell growth, and amphotericin B sensitivity, the 3–6 mutation also impairs the ability of LDL to simulate esterification and suppress HMG-CoA reductase (18). This observation suggests that the bulk of LDL-cholesterol is transported to the plasma membrane prior to eliciting homeostatic responses or shuttling to the cell interior. These data are consistent with the model of Xu and Tabas (51) that lipoprotein-cholesterol moves to the cell interior when the plasma membrane capacity to hold cholesterol is exceeded.

The mechanism of sterol transport from the cell surface to the ER has not been elucidated. Work by Skiba et al. (52) demonstrated that sphingomyelinase-stimulated cholesterol esterification is an energy-independent process. These findings distinguish the sphingomyelinase pathway from the lipoprotein-induced cholesterol esterification pathway, which is energy-dependent.

The 3–6 mutation may affect transport in several different ways. First, the cholesterol domain structure of the plasma membrane may be altered, as mentioned above. Caveolae represent one possible lateral domain, which we probed with cholesterol oxidase and found to be normal. Nevertheless, altered lateral or bilayer distribution could render cells amphotericin B-resistant and perhaps prevent cholesterol from interacting with its transport vehicle.

Second, the 3-6 mutation could also alter a cholesterol transport molecule (i.e., soluble carrier or vesicle component), although it is more difficult to envision how an impaired soluble transporter could result in amphotericin B resistance. One possibility is that cholesterol moves from the cell surface normally but remains sequestered within a cholesterol oxidase-sensitive intracellular pool, unable to mobilize further.

Lastly, the cytoskeletal network could be altered. This possibility is raised because 3-6 cells have the biochemical phenotype of human SW-13 adrenal tumor cells lacking a vimentin intermediate filament network (53). Vimentin intermediate filaments have been linked to the metabolism of lipid droplets in steroidogenic cells, but possible roles in cholesterol trafficking have not been explained (54). Mutant 3-6 cells have a normal vimentin intermediate filament network, as assessed by immunofluorescence and two-dimensional gel electrophoresis (R. M. Evans, personal communication). Nevertheless, assembly and function of other cytoskeletal components in 3-6 remains to be established.

The above arguments are examples of how a single gene defect could alter both cholesterol transport and amphotericin B sensitivity. The characterization of this mutant cell line provides an important tool for the study of cholesterol transport. Mutant 3-6 cells will not only be useful in the identification of gene products involved in the plasma membrane to ER cholesterol transport pathway by cloning methods, but will also facilitate the identification of transport pathways and homeostatic re-

sponses that do not require this inward movement of cholesterol. Finally, the mutant line may be used to increase our understanding of how cholesterol is organized into plasma membrane domains.

We thank Jerry R. Faust and Judeth J. Klansek for helpful discussions and critical reading of the manuscript. We thank Robert Evans for evaluation of the intermediate filament network. This work was supported by grants to Laura Liscum from the American Heart Association–Parke Davis and the National Institutes of Health (DK49564) and by grants to Margaret Kielian from the American Cancer Society (VM-41B) and the Hirschl Charitable Trust, by the Jack K. and Helen B. Lazar fellowship in Cell Biology, and by Cancer Center Core Support Grant NIH/NCI P30-CA13330. Fluorescence microscopy was made possible by the Center for Gastroenterology Research on Absorptive and Secretory Processes (NIDDK P30 DK34928). N. L. J. was supported by a grant from the Lucille P. Markey Charitable Trust. B. A. was supported by a National Institutes of Health Training Grant (HL07785). K. W. U. was supported by National Institutes of Health Training Grant (DK07542).

Manuscript received 9 April 1997 and in revised form 16 June 1997.

REFERENCES

1. Lange, Y. 1991. Disposition of intracellular cholesterol in human fibroblasts. *J. Lipid Res.* **32:** 329–339.
2. Warnock, D. E., C. Roberts, M. S. Lutz, W. A. Blackburn, W. W. Young, and J. U. Baenziger. 1993. Determination of plasma membrane lipid mass and composition in cultured Chinese hamster ovary cells using high gradient magnetic affinity chromatography. *J. Biol. Chem.* **268:** 10145–10153.
3. Slotte, J. P., and E. L. Bierman. 1988. Depletion of plasma membrane sphingomyelin rapidly alters the distribution of cholesterol between plasma membranes and intracellular cholesterol pools in cultured fibroblasts. *Biochem. J.* **250:** 653–658.
4. Slotte, J. P., G. Hedstrom, S. Rannstrom, and S. Ekman. 1989. Effects of sphingomyelin degradation on cell cholesterol oxidizability and steady-state distribution between the cell surface and the cell interior. *Biochim. Biophys. Acta.* **985:** 90–96.
5. Okwu, A. K., X-X. Xu, Y. Shiratori, and I. Tabas. 1994. Regulation of the threshold for lipoprotein-induced acyl-CoA:cholesterol *O*-acyltransferase stimulation in macrophages by cellular sphingomyelin content. *J. Lipid Res.* **35:** 644–655.
6. Wattenberg, B. W., and D. F. Silbert. 1983. Sterol partitioning among intracellular membranes. Testing a model for cellular sterol distribution. *J. Biol. Chem.* **258:** 2284–2289.
7. DeGrella, R. F., and R. D. Simoni. 1982. Intracellular transport of cholesterol to the plasma membrane. *J. Biol. Chem.* **257:** 14256–14262.
8. Lange, Y., F. Echevarria, and T. Steck. 1991. Movement of zymosterol, a precursor of cholesterol, among three membranes in human fibroblasts. *J. Biol. Chem.* **266:** 21439–21443.
9. Johnson, W. J., G. K. Chacko, M. C. Philips, and G. H. Rothblat. 1990. The efflux of lysosomal cholesterol from cells. *J. Biol. Chem.* **265:** 5546–5553.
10. Lange, Y., F. Strebel, and T. L. Steck. 1993. Role of the plasma membrane in cholesterol esterification in rat hepatoma cells. *J. Biol. Chem.* **268:** 13838–13843.
11. Dahl, N. K., K. L. Reed, M. A. Daunais, J. R. Faust, and L. Liscum. 1992. Isolation and characterization of Chinese hamster ovary cells defective in the intracellular metabolism of LDL-derived cholesterol. *J. Biol. Chem.* **267:** 4889–4896.
12. Pentchev, P. G., M. E. Comly, H. S. Kruth, M. T. Vanier, D. A. Wenger, S. Patel, and R. O. Brady. 1985. A defect in cholesterol esterification in Niemann-Pick disease (type C) patients. *Proc. Natl. Acad. Sci. USA.* **82:** 8247–8251.
13. Liscum, L., and J. R. Faust. 1987. Low density lipoprotein (LDL)-mediated suppression of cholesterol synthesis and LDL uptake is defective in Niemann-Pick type C fibroblasts. *J. Biol. Chem.* **262:** 17002–17008.
14. Pentchev, P. G., M. E. Comly, H. S. Kruth, T. Tokoro, J. Butler, J. Sokol, M. Filling-Katz, J. M. Quirk, D. C. Marshall, S. Patel, M. T. Vanier, and R. O. Brady. 1987. Group C Niemann-Pick disease: faulty regulation of low-density lipoprotein uptake and cholesterol storage in cultured fibroblasts. *FASEB J.* **1:** 40–45.
15. Liscum, L., R. M. Ruggiero, and J. R. Faust. 1989. The intracellular transport of low density lipoprotein-derived cholesterol is defective in Niemann-Pick Type C fibroblasts. *J. Cell Biol.* **108:** 1625–1636.
16. Carstea, E. D., M. H. Polymeropoulos, C. C. Parker, S. D. Detera-Wadleigh, R. R. O'Neill, M. C. Patterson, E. Goldin, H. Xiao, R. E. Straub, M. T. Vanier, R. O. Brady, and P. G. Pentchev. 1993. Linkage of Niemann-Pick disease type C to human chromosome 18. *Proc. Natl. Acad. Sci. USA.* **90:** 2002–2004.
17. Cadigan, K. M., D. M. Spillane, and T-Y. Chang. 1990. Isolation and characterization of Chinese hamster ovary cell mutants defective in intracellular low density lipoprotein-cholesterol trafficking. *J. Cell Biol.* **110:** 295–308.
18. Dahl, N. K., M. A. Daunais, and L. Liscum. 1994. A second complementation class of cholesterol transport mutants with a variant Niemann-Pick type C phenotype. *J. Lipid Res.* **35:** 1839–1849.
19. Goldstein, J. L., S. K. Basu, and M. S. Brown. 1983. Receptor-mediated endocytosis of low-density lipoprotein in cultured cells. *Methods Enzymol.* **98:** 241–260.
20. Faust, J. R., J. L. Goldstein, and M. S. Brown. 1977. Receptor-mediated uptake of low density lipoprotein and utilization of its cholesterol for steroid synthesis in cultured mouse adrenal cells. *J. Biol. Chem.* **252:** 4861–4871.
21. Lowry, O. H., N. J. Rosebrough, A. L. Farr, and R. J. Randall. 1951. Protein measurement with the Folin phenol reagent. *J. Biol. Chem.* **193:** 265–275.
22. Liscum, L. 1990. Pharmacological inhibition of the intracellular transport of low-density lipoprotein-derived cholesterol in Chinese hamster ovary cells. *Biochim. Biophys. Acta.* **1045:** 40–48.
23. Blanchette-Mackie, E. J., N. K. Dwyer, L. M. Amende, H. S. Kruth, J. D. Butler, J. Sokol, M. E. Comly, M. T. Vanier, J. T. August, R. O. Brady, and P. G. Pentchev. 1988. Type-C Niemann-Pick disease: low density lipoprotein uptake is associated with premature cholesterol accumulation in the Golgi complex and excessive cholesterol storage in lysosomes. *Proc. Natl. Acad. Sci. USA.* **85:** 8022–8026.

24. Bligh, E. G., and W. J. Dyer. 1959. A rapid method of total lipid extraction and purification. *Can. J. Biochem. Physiol.* **37:** 911–917.
25. Esko, J. D., and C. R. H. Raetz. 1980. Mutants of Chinese hamster ovary cells with altered membrane phospholipid composition. Replacement of phosphatidylinositol by phosphatidylglycerol in a myo-inositol auxotroph. *J. Biol. Chem.* **255:** 4474–4480.
26. Zhou, X., and G. Arthur. 1992. Improved procedures for the determination of lipid phosphorus by malachite green. *J. Lipid Res.* **33:** 1233–1236.
27. Liscum, L., and G. J. Collins. 1991. Characterization of Chinese hamster ovary cells that are resistant to 3-β-[2-(diethylamino)ethoxy] androst-5-en-17-one inhibition of low density lipoprotein-derived cholesterol metabolism. *J. Biol. Chem.* **266:** 16599–16606.
28. Marquardt, M. T., and M. Kielian. 1996. Cholesterol-depleted cells that are relatively permissive for Semliki Forest virus infection. *Virology.* **224:** 198–205.
29. Porn, M. I., and J. P. Slotte. 1990. Reversible effects of sphingomyelin degradation on cholesterol distribution and metabolism in fibroblasts and transformed neuroblastoma cells. *Biochem. J.* **271:** 121–126.
30. Smart, E. J., Y-S. Ying, P. A. Conrad, and R. G. W. Anderson. 1994. Caveolin moves from caveolae to the Golgi apparatus in response to cholesterol oxidation. *J. Cell Biol.* **127:** 1185–1197.
31. Brown, M. S., and J. L. Goldstein. 1980. Multivalent feedback regulation of HMG-CoA reductase, a control mechanism coordinating isoprenoid synthesis and cell growth. *J. Lipid Res.* **21:** 505–517.
32. Mosley, S. T., M. S. Brown, R. G. W. Anderson, and J. L. Goldstein. 1983. Mutant clone of Chinese hamster ovary cells lacking 3-hydroxy-3-methylglutaryl coenzyme A reductase. *J. Biol. Chem.* **258:** 13875–13881.
33. Schorderet, D. F., E. A. Keitges, P. M. DuBois, and S. M. Gartler. 1988. Inactivation and reactivation of sex-linked steroid sulfatase gene in murine cell culture. *Somatic Cell Mol. Genet.* **14:** 113–121.
34. Shapiro, L. J. 1989. Steroid sulfatase deficiency and X-linked ichthyosis. *In* The Metabolic Basis of Inherited Disease. C. R. Scriver, A. L. Beaudet, W. S. Sly, and D. Valle, editors. McGraw-Hill, New York. 1945–1964.
35. Harmala, A-S., M. I. Porn, P. Mattjus, and J. P. Slotte. 1994. Cholesterol transport from plasma membranes to intracellular membranes is inhibited by 3β-[2-(diethylamino)ethoxy]androst-5-en-17-one. *Biochim. Biophys. Acta.* **1211:** 317–325.
36. Goldstein, J. L., J. R. Faust, J. H. Dygos, R. J. Chorvat, and M. S. Brown. 1978. Inhibition of cholesteryl ester formation in human fibroblasts by an analogue of 7-ketocholesterol and by progesterone. *Proc. Natl. Acad. Sci. USA.* **75:** 1877–1881.
37. Cheng, D., C. C. Y. Chang, X-m. Qu, and T-Y. Chang. 1995. Activation of acyl-coenzyme A:cholesterol acyltransferase by cholesterol or by oxysterol in a cell-free system. *J. Biol. Chem.* **270:** 685–695.
38. Underwood, K. W., B. Andemariam, G. L. McWilliams, and L. Liscum. 1996. Quantitative analysis of hydrophobic amine inhibition of intracellular cholesterol transport. *J. Lipid Res.* **37:** 1556–1568.
39. Lange, Y., M. H. Swaisgood, B. V. Ramos, and T. L. Steck. 1989. Plasma membranes contain half the phospholipid and 90% of the cholesterol and sphingomyelin in cultured human fibroblasts. *J. Biol. Chem.* **264:** 3786–3793.
40. Kielian, M. 1995. Membrane fusion and the alphavirus life cycle. *Adv. Virus Res.* **45:** 113–151.
41. Kielian, M. C., and A. Helenius. 1984. The role of cholesterol in the fusion of Semliki Forest virus with membranes. *J. Virol.* **52:** 281–283.
42. Phalen, T., and M. Kielian. 1991. Cholesterol is required for infection by Semliki Forest virus. *J. Cell Biol.* **112:** 615–623.
43. Marquardt, M. T., T. Phalen, and M. Kielian. 1993. Cholesterol is required in the exit pathway of Semliki Forest virus. *J. Cell Biol.* **123:** 57–65.
44. White, J., J. Kartenbeck, and A. Helenius. 1980. Fusion of Semliki Forest virus with the plasma membrane can be induced by low pH. *J. Cell Biol.* **87:** 264–272.
45. Kinsky, S. C. 1970. Antibiotic interaction with model membranes. *Annu. Rev. Pharmacol.* **10:** 119–142.
46. Norman, A. W., R. A. Demel, B. De Kruyeff, and L. L. M. Van Deenen. 1972. Studies on the biological properties of polyene antibiotics. Evidence for the direct interaction of filipin with cholesterol. *J. Biol. Chem.* **247:** 1918–1929.
47. De Kruijff, B. 1990. Cholesterol as a target for toxins. *Biosci. Rep.* **10:** 127–130.
48. Saito, Y., S. M. Chou, and D. F. Silbert. 1977. Animal cell mutants defective in sterol metabolism: a specific selection procedure and partial characterization of defects. *Proc. Natl. Acad. Sci. USA.* **74:** 3730–3734.
49. Hidaka, K., H. Endo, S. Akiyama, and M. Kuwano. 1978. Isolation and characterization of amphotericin B-resistant cell lines in Chinese hamster cells. *Cells.* **14:** 415–421.
50. White, J., and A. Helenius. 1980. pH-Dependent fusion between the Semliki Forest virus membrane and liposomes. *Proc. Natl. Acad. Sci. USA.* **77:** 3273–3277.
51. Xu, X-X., and I. Tabas. 1991. Lipoproteins activate acyl-coenzyme A:cholesterol acyltransferase in macrophages only after cellular cholesterol pools are expanded to a critical threshold level. *J. Biol. Chem.* **266:** 17040–17048.
52. Skiba, P. J., X. Zha, F. R. Maxfield, S. L. Schissel, and I. Tabas. 1996. The distal pathway of lipoprotein-induced cholesterol esterification, but not sphingomyelinase-induced cholesterol esterification, is energy-dependent. *J. Biol. Chem.* **271:** 13392–13400.
53. Sarria, A. J., S. R. Panini, and R. M. Evans. 1991. A functional role for vimentin intermediate filaments in the metabolism of lipoprotein-derived cholesterol in human SW-13 cells. *J. Biol. Chem.* **267:** 19455–19463.
54. Evans, R. M. 1994. Intermediate filaments and lipoprotein cholesterol. *Trends Cell Biol.* **4:** 149–151.